Proceedings of:
ASME TURBO EXPO 2001
June 4-7, 2001, New Orleans, Louisiana, USA

2001-GT-0234

FINITE ELEMENT AND TRANSFER MATRIX METHODS FOR ROTORDYNAMICS - A COMPARISON

Jorgen L. Nikolajsen
School of Engineering and Advanced Technology
Staffordshire University
Stafford, England

ABSTRACT

A quantitative comparison is made between the Finite Element Method and four variants of the Transfer Matrix Method, as applied to free vibration analysis of rotor systems. The results are as follows: The Finite Element Method is the most robust method and can identify the largest number of natural frequencies. The finite-element-based Transfer Matrix Method is the most accurate method and uses the least amount of memory. The Polynomial Transfer Matrix Method is the fastest. The Riccati Transfer Matrix Method performed well but did not live up to its superior reputation. The Lund Transfer Matrix Method also performed well except on processing speed where it fell far short of the other methods.

INTRODUCTION

The Transfer Matrix Method (TMM) for transverse vibrations of beams and shafts was developed by Myklestad [1] and Prohl [2]. The Finite Element Method (FEM) for transverse shaft vibrations was developed by Ruhl and Booker [3]. Both methods are widely used in rotordynamic analysis.

Several variants of the TMM have been developed to improve its performance. Lund's [4] method is the standard against which the newer methods are usually measured. For harmonic vibration analysis, three noteworthy variants since Lund have been the Riccati TMM, first applied to rotor systems by Horner and Pilkey [5], the polynomial TMM developed by Murphy and Vance [6], and the finite-element-based TMM, first documented by Firoozian and Zhu [7]. These are the methods compared in this paper.

The traditional view of the FEM and the TMM is roughly as follows: The main advantage of the FEM over the TMM is numerical stability, allowing analysis of more complex systems and calculation of more natural frequencies. The main advantage of the TMM over the FEM is high processing speed and low memory requirements. When several TMM variants are considered, this traditional view becomes too simplistic. A more accurate and comprehensive picture is presented in this paper based on quantitative comparisons in terms of accuracy, numerical stability, processing speed, and memory requirements for a free vibration analysis of a simple shaft system.

NOMENCLATURE

e = size of largest polynomial coefficient discarded
E = Young's modulus for shaft material
I = second moment of area for shaft cross section
k = shaft support stiffness
ℓ = length of shaft element
L = total length of shaft
M = bending moment at shaft station
n = number of shaft elements
V = shear force at shaft station
y = transverse shaft displacement
γ = shaft mass per unit length
θ = angular shaft displacement
ω_c = calculated natural frequency of shaft
ω_e = 'exact' natural frequency of shaft
'bar' notation: nondimensional quantity

SYSTEM MODEL

The FEM/TMM comparisons in this paper are made for the plane motion of a simple uniform shaft with identical spring supports k at both ends, see Figure 1. Also shown in Fig. 1 is the discretization procedure used throughout the paper, i.e., the

shaft is divided into elements of equal length l. In all the TMMs, masses of size γl are lumped at the element intersections and masses of size $\gamma l/2$ are lumped at the two spring support locations.

The support stiffnesses are set at $k = 48EI/L^3$ throughout the paper. This is the midspan stiffness of the shaft on simple supports. It ensures that both the shaft and the support stiffnesses affect the locations of at least the lowest (and normally most important) natural frequencies.

'EXACT' NATURAL FREQUENCIES

The 'exact' non-dimensional natural frequencies $\bar{\omega}_e$ for the uniform shaft in Fig. 1 are the solutions to the transcendental equation

$$-1+\cos\bar{\lambda}(\cosh\bar{\lambda}-2\bar{\kappa}\sinh\bar{\lambda})+2\bar{\kappa}\sin\bar{\lambda}(\cosh\bar{\lambda}-\bar{\kappa}\sinh\bar{\lambda})=0 \tag{1}$$

where $\bar{\kappa}=48\bar{k}/\bar{\lambda}^3$, $\bar{k}=kL^3/(48EI)=1$ for $k=48EI/L^3$, $\bar{\lambda}^2=\bar{\omega}_e$, and $\bar{\omega}_e^2=\gamma L^4\omega_e^2/(EI)$. Equation (1) was derived based on Weaver et al. [8].

The 16 lowest natural frequencies were calculated to double-precision accuracy (15 significant digits) from Eq. (1) by means of a simple combined bisection/Newton-Raphson method, e.g. Press et al. [9]. The 16 frequencies are shown in Table 1 for $\bar{k}=1$. The accuracy of the FEM and the TMM calculations below are measured against these 'exact' frequencies.

Table 1 'Exact' Nondimensional Natural Frequencies

	$\bar{\omega}_e$ for $\bar{k}=1$
1.	7.132841352626294D+00
2.	1.602380148582338D+01
3.	3.022661392040124D+01
4.	6.487998220079662D+01
5.	1.225218471687941D+02
6.	2.008306058643486D+02
7.	2.992028781512469D+02
8.	4.174531875872199D+02
9.	5.555120906416892D+02
10.	7.133487247622190D+02
11.	8.909476744254407D+02
12.	1.088300535985667D+03
13.	1.305402408763302D+03
14.	1.542250277281780D+03
15.	1.798842203014556D+03
16.	2.075176893524679D+03

FINITE ELEMENT METHOD (FEM)

One shaft finite element is shown in Figure 2. The corresponding element mass and stiffness matrices are available, for example, in Craig [10]. Assuming harmonic motion, the element mass and stiffness properties, considered separately, give rise to the following relations, written here in nondimensional form:

$$-\lambda\begin{bmatrix}156 & 22 & 54 & -13\\ & 4 & 13 & -3\\ & & 156 & -22\\ \text{Sym.} & & & 4\end{bmatrix}\begin{Bmatrix}\bar{y}_1\\ \theta_1\\ \bar{y}_2\\ \theta_2\end{Bmatrix}=\begin{Bmatrix}\bar{V}_1\\ \bar{M}_1\\ \bar{V}_2\\ \bar{M}_2\end{Bmatrix} \tag{2}$$

and

$$\begin{bmatrix}12+\hat{k} & 6 & -12 & 6\\ & 4 & -6 & 2\\ & & 12+\hat{k} & -6\\ \text{Sym.} & & & 4\end{bmatrix}\begin{Bmatrix}\bar{y}_1\\ \theta_1\\ \bar{y}_2\\ \theta_2\end{Bmatrix}=\begin{Bmatrix}\bar{V}_1\\ \bar{M}_1\\ \bar{V}_2\\ \bar{M}_2\end{Bmatrix} \tag{3}$$

$\bar{y}=y/\ell$, $\bar{M}=M\ell/(EI)$, $\bar{V}=V\ell^2/(EI)$, $\lambda=\bar{\omega}_e^2/(420n^4)$, and $\bar{\omega}_e^2=\gamma L^4\omega_e^2/(EI)$ where $\bar{\omega}_e$ are the calculated natural frequencies. For the current shaft, $\hat{k}=0$ for all elements except the first and the last for which $\hat{k}=48\bar{k}/n^3$ at matrix locations (1,1) and (3,3) respectively in Eq. (3) to account for the spring supports.

The system mass and stiffness matrices are assembled as usual from the element matrices of Eqs. (2) and (3) by the direct stiffness method, e.g. Craig [10]. For the current problem, this leads to the generalized eigenproblem $[K]\{x\}=\lambda[M]\{x\}$ with symmetric band-matrices [K] and [M]. The eigenvalues λ were found by reduction to standard form, $[A]\{x\}=\lambda\{x\}$, then reduction to tridiagonal form followed by combined QL/QR iteration. Double-precision arithmetic was used throughout.

The 16 lowest natural frequencies $\bar{\omega}_e$ were calculated for a range of shaft elements from $n=2^0=1$ through 2^1, 2^2, etc. up to $2^{12}=4096$. The number of significant digits $N=\log_{10}\left|\bar{\omega}_e/(\bar{\omega}_e-\bar{\omega}_c)\right|$ are plotted versus the number of shaft elements n in Figure 3. Due to space limitations in Fig. 3, not all the frequencies are labelled but they occur in consecutive order as implied.

Fig. 3 shows, as expected, that the accuracy of all the natural frequencies initially improves as the number of shaft elements increases. Also as expected, the lower the natural frequency, the larger the number of significant digits for a given number of shaft elements below about 100. Above 100 shaft elements, the number of significant digits starts to decrease. The frequencies deteriorate in consecutive order such

that each reaches a maximum of about 7 to 8 significant digits. A practical implication is that, with the FEM, too many shaft elements can adversely affect the accuracy of the natural frequency calculations. Note also from Fig. 3 that the 16 lowest frequencies can be calculated with a maximum of only 5 significant digits in a single run and then only within a relatively narrow range of 130 to 250 shaft elements. In practice, both the accuracy and the optimum number of elements is unknown. However, reasonable estimates can be made through trial runs with increasing number of elements while watching the digits of the frequency values settle down and become constant.

LUND TRANSFER MATRIX METHOD (LTMM)

The shaft is divided into a series of lumped masses and massless beam elements of equal length as shown in Figure 4, e.g. Steidel [11]. For the current two-dimensional analysis, the transfer matrix equations for the mass and beam elements between stations i and i+1can be written in the following nondimensional form, e.g. Steidel [11]:

$$\begin{Bmatrix} \bar{y} \\ \theta \\ \bar{M} \\ \bar{V} \end{Bmatrix}_i^* = \begin{bmatrix} 1 & 0 & 0 & 0 \\ 0 & 1 & 0 & 0 \\ 0 & 0 & 1 & 0 \\ a_{41} & 0 & 0 & 1 \end{bmatrix} \begin{Bmatrix} \bar{y} \\ \theta \\ \bar{M} \\ \bar{V} \end{Bmatrix}_i \tag{4}$$

$$\begin{Bmatrix} \bar{y} \\ \theta \\ \bar{M} \\ \bar{V} \end{Bmatrix}_{i-1} = \begin{bmatrix} 1 & 1 & 1/2 & 1/6 \\ 0 & 1 & 1 & 1/2 \\ 0 & 0 & 1 & 1 \\ 0 & 0 & 0 & 1 \end{bmatrix} \begin{Bmatrix} \bar{y} \\ \theta \\ \bar{M} \\ \bar{V} \end{Bmatrix}_i^* \tag{5}$$

where

$$a_{41} = \begin{cases} \lambda/(2n^4) - 48\bar{k}/n^3 & \text{for } i = 1 \text{ and } i = n+1 \\ \lambda/n^4 & \text{for } i = 2 \text{ to } n \end{cases} \tag{6}$$

$\bar{y}, \bar{M}$, and $\bar{V}$ are as given for Eqs. (2) and (3) and $\lambda = \bar{\omega}_e^2$.

The natural frequencies $\bar{\omega}_e$ can be found by multiplying together the transfer matrices of Eqs. (4) and (5) for consecutive elements along the entire shaft to obtain the following relation between the state variables at each end of the shaft :

$$\begin{Bmatrix} \{x\} \\ \{F\} \end{Bmatrix}_{n+1} = \begin{bmatrix} [A_1] & [A_2] \\ [A_3] & [A_4] \end{bmatrix} \begin{Bmatrix} \{x\} \\ \{F\} \end{Bmatrix}_1 \tag{7}$$

where $\{x\} = \{\bar{y}, \theta\}^T$ and $\{F\} = \{\bar{M}, \bar{V}\}^T$. Boundary conditions $\{F\}_1 = \{F\}_{n+1} = 0$ dictate that the determinant $|A_3|$ must equal zero to ensure nontrivial solutions, thus, $\lambda = \bar{\omega}_e^2$ can be found as the roots of the corresponding polynomial $|A_3(\lambda)| = 0$. Since only $[A_3]$ is needed, the number of arithmetic operations can be halved by determining only $[[A_1],[A_3]]^T$. This is done by two multiplication sweeps through the shaft for given λ with initial conditions $\{y, \theta, M, V\}_1^T$ equal to $\{1,0,0,0\}^T$ and $\{0,1,0,0\}^T$ respectively. The result may be written

$$[A_3] = \begin{bmatrix} d_{31} & d_{32} \\ d_{41} & d_{42} \end{bmatrix} \tag{8}$$

Lund [4] chose Newton's method, e.g. Press et al. [9], to solve for λ. The procedure is as follows: Values for both $|A_3|$ and $d|A_3|/d\lambda$ are required. $|A_3|$ is found as above. $d|A_3|/d\lambda$ is found by differentiation of Eqs. (4) and (5) with respect to λ followed by multiplication sweeps for given λ with initial conditions $\{y, \theta, M, V, dy/d\lambda, d\theta/d\lambda, dM/d\lambda, dV/d\lambda\}_1^T = \{1,0,0,0,0,0,0,0\}^T$ and $\{0,1,0,0,0,0,0,0\}^T$ respectively. The result may be written

$$[A_3'] = \begin{bmatrix} d_{31}' & d_{32}' \\ d_{41}' & d_{42}' \end{bmatrix} \tag{9}$$

from which, in accordance with Sokolnikoff and Redheffer [12],

$$d|A_3|/d\lambda = \begin{vmatrix} d_{31}' & d_{32} \\ d_{41}' & d_{42} \end{vmatrix} + \begin{vmatrix} d_{31} & d_{32}' \\ d_{41} & d_{42}' \end{vmatrix} \tag{10}$$

Newton's method can now be applied.

In the current implementation, the more efficient and robust Laguerre method, e.g. Press et al. [9], is used. This prevents the original choice of Newton's method from unfairly reducing the efficiency of the LTMM in comparison with the methods discussed later.

Laguerre's method requires $d^2|A_3|/d\lambda^2$ also and the following expression can be derived from Eq. (10):

$$d^2|A_3|/d\lambda^2 = \begin{vmatrix} d_{31}'' & d_{32} \\ d_{41}'' & d_{42} \end{vmatrix} + 2\begin{vmatrix} d_{31}' & d_{32}' \\ d_{41}' & d_{42}' \end{vmatrix} + \begin{vmatrix} d_{31} & d_{32}'' \\ d_{41} & d_{42}'' \end{vmatrix} \tag{11}$$

The elements of

$$[A_3''] = \begin{bmatrix} d_{31}'' & d_{32}'' \\ d_{41}'' & d_{42}'' \end{bmatrix} \tag{12}$$

are needed for substitution into Eq. (11). They are found analogously to the elements of $[A_3']$ above.

The 16 lowest natural frequencies $\bar{\omega}_e$ were calculated for a range of shaft elements from $n = 2^2 = 4$ through 2^3, 2^4, etc. up to $2^{15} = 32768$. Numerical breakdown occurred at $2^{16} = 65536$ elements. The number of significant digits $N = \log_{10}|\bar{\omega}_e/(\bar{\omega}_e - \bar{\omega}_c)|$ are plotted versus the number of shaft elements n in Figure 5. Due to space limitations in Fig. 5, not all the frequencies are labelled but they occur in consecutive order as implied.

Fig. 5 confirms the expected steady increase in accuracy for increasing number of shaft elements and also the expected lower accuracy of the higher natural frequencies for a given number of elements. As the number of shaft elements grows, the accuracy levels off and becomes somewhat erratic, starting with the higher frequencies. However, the levelled-off accuracies appear to remain within about one significant digit of their former maximum values. Thus, in contrast to the FEM (Fig. 3), the overall accuracy provided by the LTMM does not deteriorate catastrophically for large numbers of shaft elements. Figs. 3 and 5 also show that the LTMM requires between 1 and 2 orders of magnitude more elements than the FEM to achieve the same accuracy. This, of course, reflects the LTMM's lumped mass discretization versus the FEM's more accurate distributed mass model. Figs. 3 and 5 also show that the FEM can identify all 16 frequencies, whereas, the LTMM only finds the 12 lowest, and the 12th only with about 3 significant digits. On the other hand, the LTMM finds the lower frequencies with better accuracy than the FEM.

POLYNOMIAL TRANSFER MATRIX METHOD (PTMM)

The PTMM uses the same transfer matrix model and the same transfer matrix equations as the LTMM, see Fig. 4 and Eqs (4) and (5). However, the PTMM determines the polynomial coefficients of the determinant $|A_3(\lambda)|$, corresponding to Eq. (8), explicitly once and for all for a particular rotor system, e.g. Vance [13]. The polynomial roots $\lambda = \bar{\omega}_e^2$ are then extracted using one of the many available polynomial root solvers, e.g. Press et al. [9]. Thus, the PTMM requires only a single set of transfer matrix sweeps of the shaft. For comparison, the LTMM works directly with the determinant value $|A_3|$ and its derivatives and requires one set of sweeps for each iteration step for each natural frequency. The PTMM has the potential for providing significant gains in efficiency at the cost of some loss of robustness, e.g., (1) the polynomial coefficients become so large that scaling is required to prevent overflow, and (2) the polynomial order becomes so large that truncation of the higher order terms is needed before root extraction to maximize efficiency. This calls for some cognizance on the part of the user.

The current PTMM implementation is relatively simple, using only a single scaling operation before the polynomial coefficient evaluation and a single truncation operation at the end of the polynomial coefficient evaluation. This was considered sufficient for comparison with the subsequent TMMs which have similar implementations. Both Laguerre's method and Bairstow's method were tried as root extractors, e.g. Press et al. [9]. There was little difference between them in terms of efficiency so the slightly simpler Bairstow's method was chosen; also because of its traditional connection with the PTMM. (This choice is not available for the LTMM since Bairstow's method requires access to explicit values for the polynomial coefficients).

The 16 lowest natural frequencies $\bar{\omega}_e$ were calculated for a range of shaft elements from $n = 2^2 = 4$ through 2^3, 2^4, etc. up to $2^{15} = 32768$. Numerical breakdown occurred at $2^{16} = 65536$ elements. The number of significant digits $N = \log_{10}|\bar{\omega}_e/(\bar{\omega}_e - \bar{\omega}_c)|$ are plotted versus the number of shaft elements n in Figure 6. Polynomial coefficients with absolute values smaller than $e = 10^{-125}$ have been discarded. $e \approx 10^{-125}$ was found to be roughly the maximum coefficient value which could be discarded without losing significant digits. The results are almost identical to the LTMM results in Fig. 5, with a slight advantage to the PTMM. Thus, the previous discussion of Fig. 5 applies to Fig. 6 also. The two methods appear to have almost identical accuracy and stability characteristics.

RICCATI TRANSFER MATRIX METHOD (RTMM)

The RTMM uses the same transfer matrix model and the same transfer matrix equations as the LTMM and the PTMM, see Fig. 4 and Eqs (4) and (5). Eqs. (4) and (5) are rewritten in terms of sub-matrices as follows:

$$\begin{Bmatrix}\{x\}\\ \{F\}\end{Bmatrix}_i^* = \begin{bmatrix}[I] & [0]\\ [K_i] & [I]\end{bmatrix}\begin{Bmatrix}\{x\}\\ \{F\}\end{Bmatrix}_i \text{ and } \begin{Bmatrix}\{x\}\\ \{F\}\end{Bmatrix}_{i+1} = \begin{bmatrix}[L_i] & [B_i]\\ [0] & [L_i]\end{bmatrix}\begin{Bmatrix}\{x\}\\ \{F\}\end{Bmatrix}_i^* \quad (13)$$

where $\{x\} = \{\bar{y}, \theta\}^T$ and $\{F\} = \{\bar{M}, \bar{V}\}^T$. The recursive formulas

$$\begin{cases}[R_i] = [L_{i-1}][R_{i-1}] + [B_{i-1}][P_{i-1}]\\ [P_i] = [K_i][R_i] + [L_{i-1}][P_{i-1}]\end{cases} \quad (14)$$

can be derived from Eqs (13) with $[R_1] = [I]$ and $[P_1] = [K_1]$ and the natural frequencies $\bar{\omega}_e$ can be found by equating the determinant $|P_{n+1}(\lambda)|$ to zero, e.g. Songuyan [14].

The matrix order of Eqs. (14) is reduced by half compared to Eqs. (13). The objective is to improve the numerical stability and reduce the computational time and storage requirements, as discussed by for example Horner and Pilkey [5] and Songuyan [14]. The RTMM was implemented here using a PTMM-type

algorithm to determine the polynomial coefficients once and for all, then solving for the polynomial roots λ using Bairstow's method.

The 16 lowest natural frequencies $\overline{\omega}_c$ were calculated for a range of shaft elements from $n = 2^2 = 4$ through 2^3, 2^4, etc. up to $2^{15} = 32768$. Numerical breakdown occurred at $2^{16} = 65536$ elements. The number of significant digits $N = \log_{10}\left|\overline{\omega}_e/(\overline{\omega}_e - \overline{\omega}_c)\right|$ are plotted versus the number of shaft elements n in Figure 7. Polynomial coefficients with absolute values smaller than $e = 10^{-125}$ have been discarded. $e \approx 10^{-125}$ was found to be roughly the maximum coefficient value which could be discarded without losing significant digits. The results are virtually identical to the PTMM results in Fig. 6. Thus, no improvement in accuracy or stability of the RTMM over the PTMM was detected in the current study.

FINITE-ELEMENT-BASED TRANSFER MATRIX METHOD (FETMM)

The FETMM is based on the finite element model of Eqs. (2) and (3). The idea is to rearrange Eqs. (2) and (3) to obtain state-variables of the type $\{y, \theta, M, V\}_i^T$, thus, turning the finite element formulation into a transfer matrix formulation with superior accuracy due to the distributed mass modeling, see Firoozian and Zhu [7].

Eqs. (2) and (3) can be added and re-arranged into

$$\begin{Bmatrix} \overline{y} \\ \theta \\ \overline{M} \\ \overline{V} \end{Bmatrix}_{i+1} = \frac{1}{d}\left[\begin{array}{cc|cc} b_{11} & b_{12} & a_3 & a_4 \\ b_{21} & b_{22} & a_6 & a_3 \\ \hline c_{11} & c_{12} & b_{22} & b_{12} \\ c_{21} & c_{11} & b_{21} & b_{11} \end{array}\right] \begin{Bmatrix} \overline{y} \\ \theta \\ \overline{M} \\ \overline{V} \end{Bmatrix}_i \qquad (15)$$

where $b_{11} = a_1a_3 - a_4a_5$, $b_{12} = a_2a_3 - a_1a_4$, $b_{21} = a_1a_6 - a_3a_5$,
$b_{22} = a_2a_6 - a_1a_3$, $c_{11} = a_3d - a_1b_{11} + a_2b_{21}$,
$c_{12} = a_4d - a_1b_{12} + a_2b_{22}$, $c_{21} = a_6d - a_5b_{11} + a_1b_{21}$,
$a_1 = 6 - 22\lambda$, $a_2 = 4 - 4\lambda$, $a_3 = 6 + 13\lambda$, $a_4 = 2 + 3\lambda$,
$a_5 = 12 - 156\lambda$, $a_6 = 12 + 54\lambda$, and $d = 12 + 12\lambda + 7\lambda^2$.

λ and $\{\overline{y}, \theta, \overline{M}, \overline{V}\}^T$ are defined as for the FEM above. The sign conventions of Fig. 4 apply. Support stiffnesses $\hat{k}$ are accounted for by replacing state-variable $\overline{V}$ by $\overline{V} - \hat{k}\overline{y}$ at the support stations.

The FETMM was implemented using a PTMM-type algorithm to determine the polynomial coefficients once and for all, then solving for the polynomial roots λ using Bairstow's method. The polynomial order is roughly twice that of the PTMM because of the heavier dependence on λ of the matrix elements of Eq. (15). The common factor 1/d in Eq. (15) can be ignored in the current free vibration analysis.

The 16 lowest natural frequencies $\overline{\omega}_c$ were calculated for a range of shaft elements from $n = 2^1$, 2^2, 2^3, etc. up to $n = 2^8 = 256$. Numerical breakdown occurred at $n = 2^9 = 512$ elements. The number of significant digits $N = \log_{10}\left|\overline{\omega}_e/(\overline{\omega}_e - \overline{\omega}_c)\right|$ are plotted versus the number of shaft elements n in Figure 8. Polynomial coefficients with absolute values smaller than $e = 10^{-125}$ have been discarded. $e \approx 10^{-125}$ was again found to be roughly the maximum coefficient value which could be discarded without sacrificing significant digits.

Fig. 8 shows that the FETMM has the same steep rise in accuracy with increasing number of shaft elements as the FEM (compare Fig. 3). However, the FETMM maintains the steep rise in accuracy for much longer than the FEM. It is able to deliver the 1st natural frequency with 11 significant digits compared to 8 for the FEM and about 9½ for the PTMM, see Figs. 3 and 6. However, the superior accuracy, relative to the PTMM, fades slowly for higher frequencies and vanishes at the 7th natural frequency. Higher frequencies are then delivered with similar but somewhat erratic accuracy by both methods. Overall, the FETMM is therefore considered to be the most accurate of the methods investigated.

COMPARISON OF EFFICIENCY

The FEM and the TMMs have been compared so far in terms of accuracy and stability. In summary, the FEM is able to deliver the most natural frequencies while the FETMM is able to provide the highest accuracy for the natural frequencies it can deliver. All the TMMs can deliver about the same number of frequencies.

The question remaining is: *which method is the fastest for providing a given number of frequencies to a given number of significant digits?*

Figure 9 is required to answer this question. It shows the processing time needed by each method to calculate the 16 lowest natural frequencies as functions of the number of shaft elements. (The PTMM graph for e = 0 is included to show how strongly the efficiency of the PTMM depends on proper polynomial truncation). The processing time was found to be almost independent of the number of natural frequencies calculated for all the methods except the LTMM. For the FEM, this is because all the frequencies are calculated irrespective of how many are requested. For the TMMs, it is because the derivation of the polynomial coefficients is far more time consuming than the subsequent extraction of the 16 polynomial roots. For the LTMM, on the other hand, the processing time is directly related to the number of natural frequencies requested, e.g., calculating 8 frequencies takes about half the time shown in Fig. 9.

The results were generated on a relatively slow 80486 33 MHz processor providing the advantage of good resolution in the processing time measurements.The FEM implementation took full advantage of the symmetry and 'bandedness' of the

system matrices. The LTMM, PTMM, and RTMM implementations took full advantage of the sparseness of the transfer matrices of Eqs. (4) and (5). No such advantage is availabe for the dense FETMM matrix of Eq. (15).

In terms of the question posed at the start of this section, the PTMM outperforms the LTMM and the RTMM because (1) all three methods have virtually identical accuracy and stability, compare Figs. 5, 6, and 7, and (2) the PTMM is faster than the RTMM and the LTMM regardless of the number of shaft elements, see Fig. 9. Therefore, only the PTMM, the FETMM and the FEM remain contenders.

Fig. 9 shows that the FEM and the FETMM have almost the same processing speed regardless of the number of shaft elements. Their overall relative merits therefore remain as outlined earlier, i.e., the FEM has superior stability and the FETMM has superior accuracy. The PTMM is unable to compete on any of these counts, compare Figs. 3, 6, and 8. The final consideration is therefore whether the PTMM can outperform the FEM and the FETMM on processing speed. This was determined by replotting Figs. 3, 6, 8, and 9 to show number of significant digits versus processing time. These figures have been omitted due to space limitations. They show that the FEM and the FETMM can provide the 1st natural frequency about 3 times faster than the PTMM regardless of the number of significant digits. However, this speed advantage diminishes as additional frequencies are requested and starts to reverse at about 3 frequencies. For 8 frequencies, the PTMM is about twice as fast as the FEM and the FETMM regardless of the number of significant digits. These findings can be roughly verified by reference to Figs. 3, 6, 8, and 9. In practice, more than 3 frequencies would usually be required, therefore, the PTMM may be regarded as the fastest of the methods tested.

Sample memory requirements were obtained from a calculation of the 8 lowest natural frequencies with 6 correct digits for the shaft system of Fig. 1. The results are summarized in Table 2 which shows that the FETMM is clearly superior in terms of memory requirements. This is due to the small number of shaft elements it needs. Note that the number of elements needed by the FEM is so low that its memory requirements fall below the TMMs' (except for the FETMM). The PTMM's and RTMM's relatively large memory requirements are due to the storage required for the polynomial coefficient calculation algorithm. Note that, in practice, a numerical grid generator would be needed to set up the 4096 elements needed by the LTMM, the PTMM, and the RTMM.

Table 2 Requirements for 8 Frequencies with 6 Correct Digits

Method	Elements	Time [s]	Memory [kB]
FEM	128	17	279
LTMM	4096	202	331
PTMM	4096	8	654
RTMM	4096	12	660
FETMM	128	23	146

Other factors influence the choice of 'best' method. For example, the FEM has the advantage of not requiring any parameter tweaking to optimize its performance. The polynomial-based TMMs require adjustment of polynomial truncation and scaling parameters to optimize their performance. Another potential drawback of the TMMs is that they provide no absolute safeguard against missing an important low frequency. This is because (1) the generated polynomial normally is too ill-conditioned to allow extraction of all the higher roots and, (2) unfortunately, no root extractor exists which can be guaranteed to find all the lower roots unless it can find all the roots.

Thus, based on the current study, there is no single winner. The method of choice appears to be the PTMM for processing speed, the FETMM for accuracy and low memory requirements, and the FEM for stability and robustness. Accuracy, stability, and robustness are considered of primary importance. Available computer power makes processing speed and memory requirements less critical except perhaps for very large rotor systems.

The relatively unfavorable findings regarding the RTMM are not supported by the literature on the RTMM known to the author. However, they seem to be confirmed by comparison of Eqs. (4) and (5) for the PTMM with Eqs. (14) for the RTMM. One set of station transfers, with Eqs. (4) and (5) combined, and with initial conditions $\{y,\theta,M,V\}_1^T = \{1,0,0,0\}^T$ and $\{0,1,0,0\}^T$, requires a maximum of 32 multiplications and 24 additions, and one evaluation of [P] from Eqs. (14) requires exactly the same number of operations. In a three-dimensional analysis, with transfer matrices of order 4x4, one set of PTMM station transfers would require 128 multiplications and 112 additions, whereas, one RTMM [P]-evaluation would require 256 multiplications and 224 additions. This suggests that the PTMM is the more efficient. The author would welcome discussions from researchers who have evidence to the contrary.

The comparisons presented in this paper are to some extent affected by the simplicity of the system analysed. For example, application of the FEM to the system in Fig. 1 leads to the eigenproblem $[K]\{x\} = \lambda[M]\{x\}$, where [K] and [M] are symmetric band-matrices with low memory requirements. Very efficient eigensolvers are available for this problem. This helps explain the surprisingly low processing time and memory requirements for the FEM, as shown in Table 2. If journal bearings were included in the FEM analysis, then an eigenproblem of the type $[[M]\lambda^2 + [B]\lambda + [K]]\{x\} = 0$ would result with nonsymmetric band-matrices and complex λ. This would typically be solved by reduction to standard form, $[A]\{x\} = \lambda\{x\}$, at twice the matrix order and with [A] nonsymmetric and non-banded. The eigensolvers available for this problem are far less efficient. In contrast, the efficiency of the polynomial TMM algorithms is much less sensitive to additional system complexities.

CONCLUSION

A quantitative comparison has been made between the Finite Element Method (FEM), the Lund Transfer Matrix Method (LTMM), the Polynomial Transfer Matrix Method (PTMM), the Riccati Transfer Matrix Method (RTMM), and the Finite-Element based Transfer Matrix Method (FETMM) in terms of free vibration analysis of a simple shaft system. The PTMM was found to be generally the fastest method. The FETMM was the most accurate and had the lowest memory requirements. The FEM could extract the most frequencies but with the lowest accuracy. The RTMM performed well but did not live up to its reputation for superior performance. The LTMM also performed well except on processing speed where it fell far short of the other methods.

REFERENCES

1. Myklestad, N.O., 1944, "A New Method for Calculating Natural Modes of Uncoupled Bending Vibration of Airplane Wings and Other Types of Beams", Journal of the Aeronautical Sciences, pp. 153-162.
2. Prohl, M.A., 1945, "A General Method for Calculating Critical Speeds of Flexible Rotors", ASME Journal of Applied Mechanics, Vol. 12, pp. A142-A148.
3. Ruhl, R.L. and Booker, J.F., 1972, "A Finite Element Model for Distributed Parameter Turborotor Systems", ASME Journal of Engineering for Industry, Vol. 94, pp. 126-132.
4. Lund, J.W., 1974, "Stability and Damped Critical Speeds of a Flexible Rotor in Fluid-Film Bearings", ASME Journal of Engineering for Industry, Vol. 96, pp. 509-517.
5. Horner, G.C. and Pilkey, W.D., 1978, "The Riccati Transfer Matrix Method", ASME Journal of Mechanical Design, Vol. 100, pp. 297-302.
6. Murphy, B.T., and Vance, J.M., 1983, "An Improved Method for Calculating Critical Speeds and Rotordynamic Stability of Turbomachinery", ASME Journal of Engineering for Power, Vol. 105, pp. 591-595.
7. Firoozian, R., and Zhu, H., 1991, "A Hybrid Method for the Vibration Analysis of Rotor-Bearing Systems", Proceeding of the IMechE, Part C: Journal of Mechanical Engineering Science, Vol. 205, pp. 131-137.
8. Weaver, W., Timoshenko, S.P., and Young, D.H., 1990, *Vibration Problems in Engineering*, 5th Ed., John Wiley, New York.
9. Press, W.H., Flannery, B.P., Teukolsky, S.A., and Vetterling, W.T., 1989, *Numerical Recipes*, Cambridge University Press, New York.
10. Craig, R.R., 1981, *Structural Dynamics. An Introduction to Computer Methods*, John Wiley, New York.
11. Steidel, R.F., 1989, *An Introduction to Mechanical Vibrations*, 3rd Ed., John Wiley, New York.
12. Sokolnikoff, I.S., and Redheffer, R.M., 1958, *Mathematics of Physics and Modern Engineering*, McGraw-Hill, New York.
13. Vance, J.M., 1988, *Rotordynamics of Turbomachinery*, John Wiley, New York.
14. Songyuan, L., 1985, "A Method for Calculating Damped Critical Speeds and Stability of Rotor-Bearing Systems", ASME Paper No. 85-DET-116, 7p.

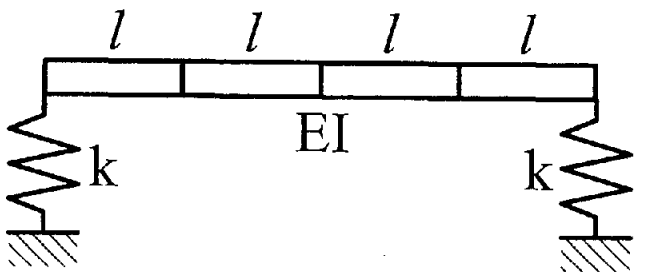

Figure 1 Uniform Shaft on Spring Supports

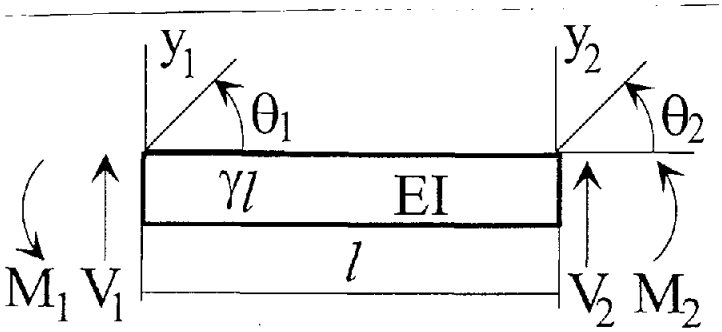

Figure 2 Shaft Finite Element

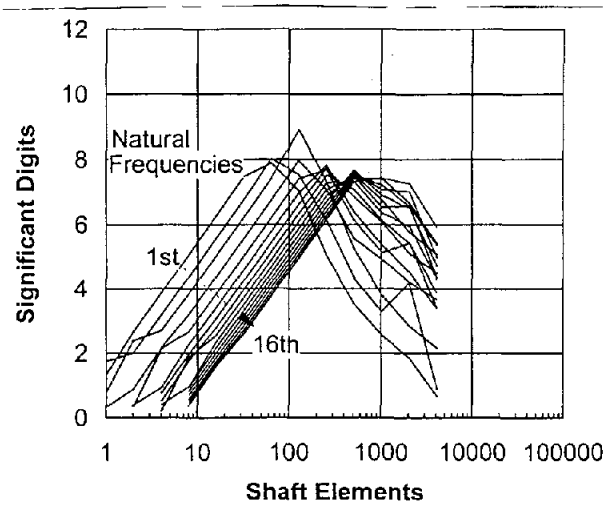

Figure 3 FEM Error Analysis

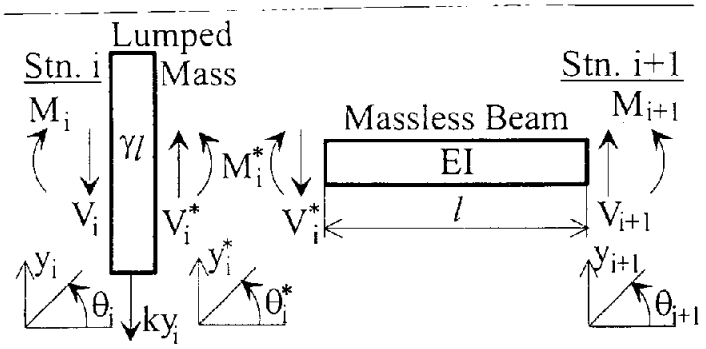

Figure 4 Shaft Transfer Matrix Elements Between Stations i and i+1

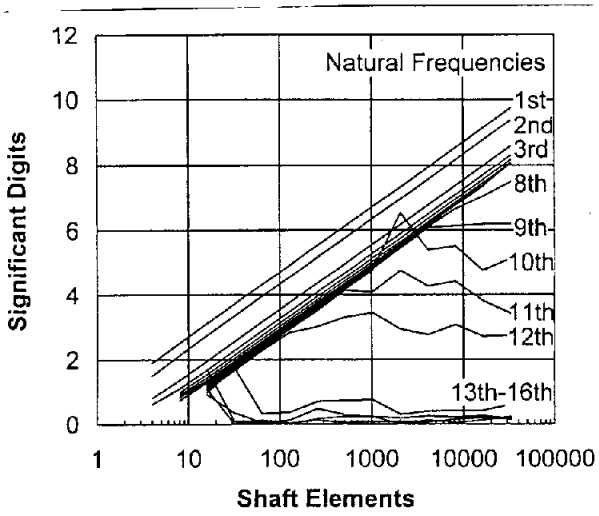

Figure 5 LTMM Error Analysis

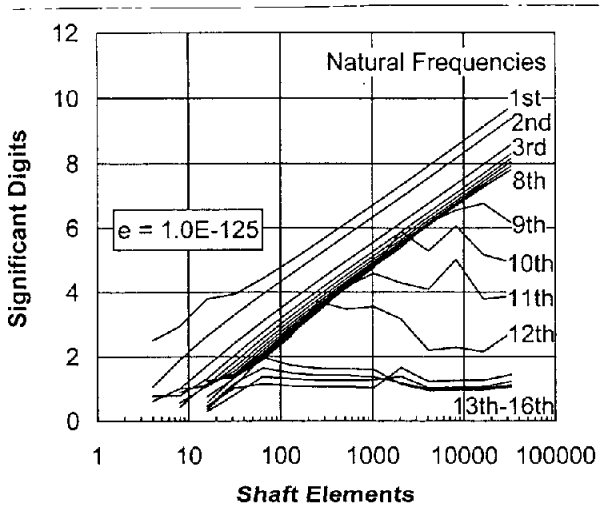

Figure 6 PTMM Error Analysis

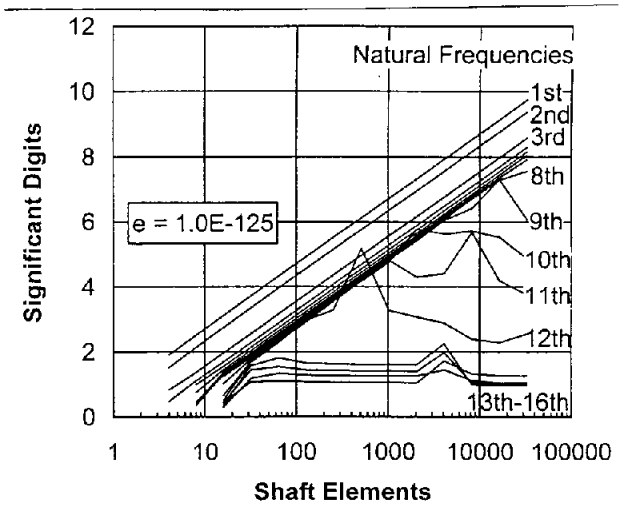

Figure 7 RTMM Error Analysis

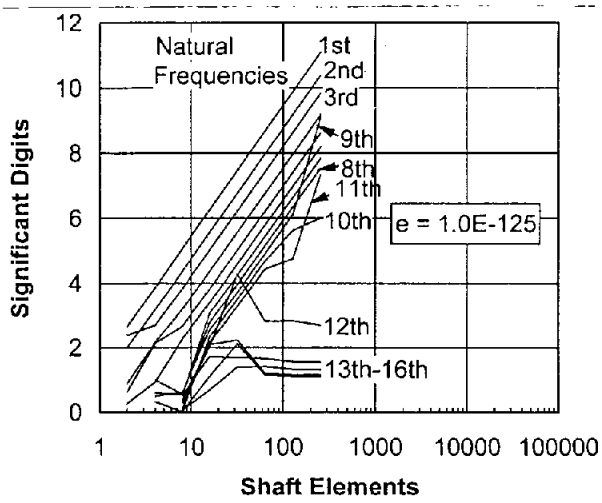

Figure 8 FETMM Error Analysis

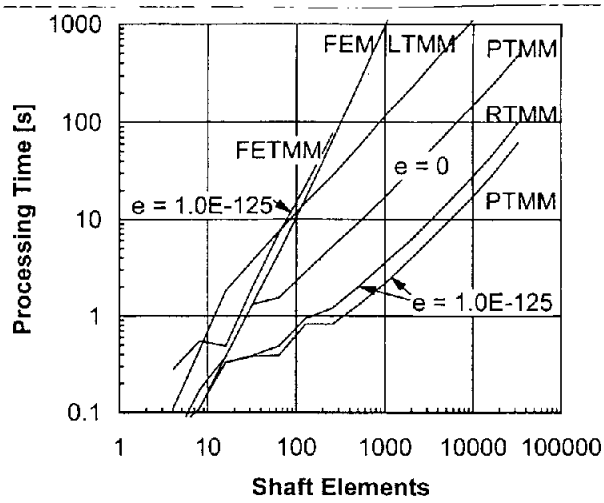

Figure 9 Processing Time for 16 Lowest Natural Frequencies